

Quantifying influence of operational parameters on photocatalytic H₂ evolution over Pt-loaded nanocrystalline mesoporous TiO₂ prepared by single-step sol–gel process with surfactant template

Thammanoon Sreethawong^{a,*}, Tarawipa Puangpetch^a,
Sumaeth Chavadej^a, Susumu Yoshikawa^b

^a The Petroleum and Petrochemical College, Chulalongkorn University, Soi Chula 12, Phayathai Road, Pathumwan, Bangkok 10330, Thailand

^b Institute of Advanced Energy, Kyoto University, Uji, Kyoto 611-0011, Japan

Received 6 November 2006; received in revised form 16 December 2006; accepted 20 December 2006

Available online 22 January 2007

Abstract

The photocatalytic evolution of hydrogen from water was investigated under various conditions over 0.6 wt% Pt-loaded nanocrystalline mesoporous TiO₂ photocatalyst prepared by a single-step sol–gel process with a surfactant template. The highly crystalline photocatalyst possessed a mesoporous characteristic with high surface area and narrow monomodal pore size distribution. More specifically, the influence of the following operational parameters, namely sacrificial reagent type, initial solution pH, photocatalyst concentration, initial sacrificial reagent concentration (of the best sacrificial reagent studied), and irradiation time, was the main focus. The hydrogen evolution was experimentally found to be strongly affected by all of the above parameters. The optimum values of initial solution pH, photocatalyst concentration, and sacrificial reagent concentration, as well as the appropriate type of sacrificial reagent, were obtained. The results showed that the utilization of the photocatalyst with the proper selection of optimum operational conditions could lead to considerably high photocatalytic hydrogen evolution activity.

© 2007 Elsevier B.V. All rights reserved.

Keywords: Photocatalysis; Hydrogen evolution; Pt/TiO₂; Single-step sol–gel; Surfactant template; Mesoporous material

1. Introduction

From the beginning of the last century, the scientific community has recognized hydrogen (H₂) as a potential source of fuel. Current uses of H₂ are generally in industrial processes, as well as in rocket fuels and spacecraft propulsion. With further research and development, this hydrogen fuel is believed to be able to effectively serve as an alternative source of energy for generating electricity and fueling motor vehicles. Therefore, it is of significant interest in the development of fuel processing technologies and catalysts/photocatalysts to produce H₂ from an abundantly available resource; water.

Efforts are currently underway to improve photochemical methods for H₂ production. Heterogeneous photocatalysis is one of the most promising approaches in this regard [1–6]. This

technique is based on the photoexcitation of a semiconductor photocatalyst with the absorption of photons of energy equal to or greater than the band gap, leading to better oxidation (formation of photogenerated holes, h_{vb}⁺) and reduction (formation of photogenerated electrons, e_{cb}⁻). The potential levels of the valence band (V_{vb}) and conduction band (V_{cb}) edges play a vital role in predicting the type of reactions that can occur at the surface of the semiconductor photocatalyst. The magnitude of these potentials depends on the nature of the solvent and the pH of the system. Another important factor that makes photocatalysis productive is the ability of the solvent to suppress the undesired electron–hole recombination, either by capturing the valence band holes or the conduction band electrons. Water is the most commonly used solvent in photocatalysis and is the most readily available chemical feedstock, as mentioned earlier, for photocatalytic H₂ evolution through water splitting. But the main associated problem is the low H₂ yield. To resolve this hindrance, primarily oxygenated hydrocarbons, such as methanol and ethanol, have been frequently employed in this water splitting

* Corresponding author. Tel.: +66 2 218 4132; fax: +66 2 215 4459.
E-mail address: thammanoon.s@chula.ac.th (T. Sreethawong).

reaction [7–16]. Due to the presence of polarity and its ability to donate the lone-pair electron, these kinds of hydrocarbons behave as a sacrificial reagent, also widely known as hole scavenger or electron donor, to prevent an unfavorable electron–hole recombination during the photoexcitation process.

Since the discovery of the photoelectrochemical splitting of water on a titanium dioxide (TiO_2) electrode [17], TiO_2 semiconductor-based photocatalysis has attracted a great deal of study, owing to its high photocatalytic activity, good stability, and non-toxic property. Although TiO_2 is superior to other semiconductors in a variety of practical uses, it still possesses a serious defect that limits its photocatalytic activity; the electron–hole recombination subsequent to the band gap excitation. The high rate of the electron–hole recombination of TiO_2 particles results in a low efficiency of photocatalysis [18]. Many attempts have been made to overcome this weak point of TiO_2 ; for example, the depositing of noble metals, especially platinum (Pt), the mixing of metal oxides with TiO_2 , and the doping of selective metal ions into the TiO_2 lattice [19–26]. The advantage of depositing noble metals is the trapping of the photogenerated charge carriers by the metal particles and thus the inhibition of their recombination during migration from inside the material to the surface. The effect of metal deposition depends on many factors, such as the metal concentration and the distribution of the metal particles [20]. For the photocatalytic H_2 evolution from water, the deposition of Pt particles on the TiO_2 surface has been shown to greatly enhance the photocatalytic production of H_2 from water/sacrificial reagent solutions, since Pt particles not only help the separation of the photogenerated species in illuminated TiO_2 but also act as H_2 evolution sites [7,18,27,28]. There have been a multitude of studies on Pt deposition onto commercially available TiO_2 powders, especially Degussa P-25, which normally possess a non-mesoporous characteristic. However, to our knowledge, investigations on Pt-deposited mesoporous TiO_2 and their photocatalytic activity for H_2 evolution have not been extensively reported.

Since the discovery by Antonelli and Ying [29] of mesoporous TiO_2 synthesized by a sol–gel process with phosphorous surfactants as templates, various methods of surfactant templating have been developed for the preparation of mesoporous structures of TiO_2 [30–32]. Since mesoporous materials normally possess large surface area and narrow pore size distribution, which advantageously make them a versatile candidate in the catalysis field, the utilization of mesoporous TiO_2 in many catalytic reactions becomes very attractive. It is generally anticipated that the use of a high surface area mesoporous oxide support rather than a commercial support for noble or transition metals has some beneficial effects on the catalytic performance. The mesoporous support would give rise to well-dispersed and stable metal particles on its surface after the steps of calcination and reduction, and as a consequence it would show an improved catalytic performance [33]. To achieve such high catalytic activity of the TiO_2 photocatalyst, attempts to focus on the synthesis step are needed, since the light harvesting capability and the reactant accessibility can be enhanced as a result of multiple scattering and high surface area, as well as uniform pore structure of the synthesized TiO_2 .

In our previous work [34], the Pt-loaded nanocrystalline mesoporous TiO_2 photocatalyst with 0.6 wt% optimum Pt loading prepared by a single-step sol–gel (SSSG) process with a surfactant template was verified for the first time to possess a superior photocatalytic performance for H_2 evolution to those prepared by conventional incipient wetness impregnation and photochemical deposition processes. The photocatalytic H_2 evolution activity of the SSSG photocatalyst was enhanced in average by about 18% in comparison with the other two processes. Following this accomplishment in the synthesis of highly photocatalytic active Pt-loaded mesoporous TiO_2 , it is essential to optimize all relevant reaction conditions, aiming at obtaining maximum H_2 evolution activity. In this contribution, the influence of various operational parameters on photocatalytic H_2 evolution was quantitatively investigated and optimized over the SSSG-prepared 0.6 wt% Pt-loaded mesoporous TiO_2 photocatalyst.

2. Experimental

2.1. Materials

Tetraisopropyl orthotitanate (TIPT, Tokyo Chemical Industry Co. Ltd.), hydrogen hexachloroplatinate (IV) hydrate (Nacalai Tesque Inc.), laurylamine hydrochloride (LAHC, Tokyo Chemical Industry Co. Ltd.), acetylacetone (ACA, Nacalai Tesque Inc.) and methanol (Nacalai Tesque Inc.) were used for the synthesis of Pt-loaded mesoporous TiO_2 . LAHC was used as a surfactant template, behaving as a mesopore-directing agent. ACA, serving as a modifying agent, was applied to moderate the hydrolysis and condensation processes of titanium precursor. HCl and NaOH (Nacalai Tesque Inc.) were used for the adjustment of the reaction solution pH. Various sacrificial reagents, including methanol, ethanol, 1-propanol, 2-propanol, 1-butanol, acetic acid, acetone, ethylene glycol, diethylene dioxane (1,4-dioxane), and dimethyl formamide (Nacalai Tesque Inc.) were comparatively utilized for the photocatalytic reaction study. All chemicals were analytical grade and were used without further purification.

2.2. Photocatalyst synthesis procedure

Single-step sol–gel (SSSG)-made 0.6 wt% Pt-loaded nanocrystalline mesoporous TiO_2 photocatalyst was synthesized via a combined sol–gel with surfactant-assisted templating mechanism in the LAHC/TIPT modified with ACA system [34]. In a typical synthesis, a specified amount of analytical grade ACA was first introduced into TIPT with a molar ratio of unity. The mixed solution was then gently shaken until homogeneous mixing. Afterwards, a 0.1 M LAHC aqueous solution of pH 4.2 was added to the ACA-modified TIPT solution, in which the molar ratio of TIPT to LAHC was tailored to a value of 4:1. The mixture was continuously stirred at room temperature for an hour and was then aged at 40 °C for 10 h to obtain transparent yellow sol-containing solution as a result of the complete hydrolysis of the TIPT precursor. To the aged TiO_2 sol solution, a specific amount of hydrogen hexachloroplatinate (IV) hydrate

in methanol was incorporated for a desired Pt loading of 0.6 wt%, and the final mixture was further aged at 40 °C for 1 day to acquire a homogeneous solution. Then, the condensation reaction-induced gelation was allowed to proceed by placing the sol-containing solution into an oven at 80 °C for a week to ensure complete gelation. Subsequently, the gel was dried overnight at 80 °C to eliminate the solvent, which was mainly the distilled water used in the preparation of the surfactant aqueous solution. The dried sample was calcined at 500 °C for 4 h to remove the LAHC template and to consequently produce the desired photocatalyst.

2.3. Photocatalyst characterizations

X-ray diffraction (XRD) was used to identify the crystalline phases present in the sample. A Rigaku RINT-2100 rotating anode XRD system generating monochromated Cu K α radiation with a continuous scanning mode at a rate of 2° min⁻¹ and operating conditions of 40 kV and 40 mA was used to obtain an XRD pattern. A nitrogen adsorption system (BEL Japan BELSORP-18 Plus) was employed to create adsorption–desorption isotherm at the liquid nitrogen temperature of –196 °C. The Brunauer–Emmett–Teller (BET) approach, using adsorption data over the relative pressure ranging from 0.05 to 0.35, was utilized to determine the surface area of the photocatalyst sample. The Barrett–Joyner–Halenda (BJH) approach was used to determine pore size distribution from the desorption data. The sample was degassed at 200 °C for 2 h to remove physisorbed gases prior to the measurement. The sample morphology was observed by a transmission electron microscope (TEM, JEOL JEM-200CX) and a scanning electron microscope (SEM, JEOL JSM-6500FE) operated at 200 and 15 kV, respectively. The elemental mappings over the desired region of the photocatalyst were detected by an energy-dispersive X-ray spectrometer (EDS) attached to the SEM.

2.4. Photocatalytic activity testing

The photocatalytic H₂ evolution reaction was performed in a closed gas-circulating system. In a typical run, a specified amount of the photocatalyst was suspended in an aqueous sacrificial reagent solution by using a magnetic stirrer within an inner irradiation reactor made of Pyrex glass. A high-pressure Hg lamp (300 W, λ_{max} of 365 nm) was utilized as the light source. The initial solution pH was adjusted to a desired value by adding a few drops of either HCl or NaOH aqueous solution with an appropriate concentration. Prior to the reaction, the mixture was left in the dark while being simultaneously thoroughly deaerated by purging the system with Ar gas for 30 min. Afterwards, the photocatalytic reaction system was closed, and the reaction was started by exposing the photoreactor to the light irradiation. To avoid heating of the solution during the course of the reaction, water was circulated through a cylindrical Pyrex jacket located around the light source. The gaseous H₂ evolved was collected at different intervals of irradiation time and was analyzed by an on-line gas chromatograph (Shimadzu GC-8A, Molecular sieve 5 Å, Ar gas), which was connected to a circulation line and

equipped with a thermal conductivity detector (TCD). Different operational parameters were quantitatively varied in order to obtain the optimum conditions for the maximum photocatalytic H₂ evolution over the Pt-loaded mesoporous TiO₂ photocatalyst. These operational parameters included sacrificial reagent type, initial solution pH, photocatalyst concentration, initial sacrificial reagent concentration (of the best sacrificial reagent), and irradiation time.

3. Results and discussion

3.1. Photocatalyst characterizations

Fig. 1 shows the nitrogen adsorption–desorption isotherm and pore size distribution of the 0.6 wt% Pt-loaded mesoporous TiO₂ photocatalyst. The isotherm in Fig. 1(a) is of typical type IV pattern with hysteresis loop, which is a marked characteristic of mesoporous materials, according to the IUPAC classification [35]. The well-defined hysteresis loop with a sloping adsorption branch and a relatively steep desorption branch belongs to H2 type. It is well known that a distribution of various sized cavities, but with the same entrance diameter, would be attributed to this

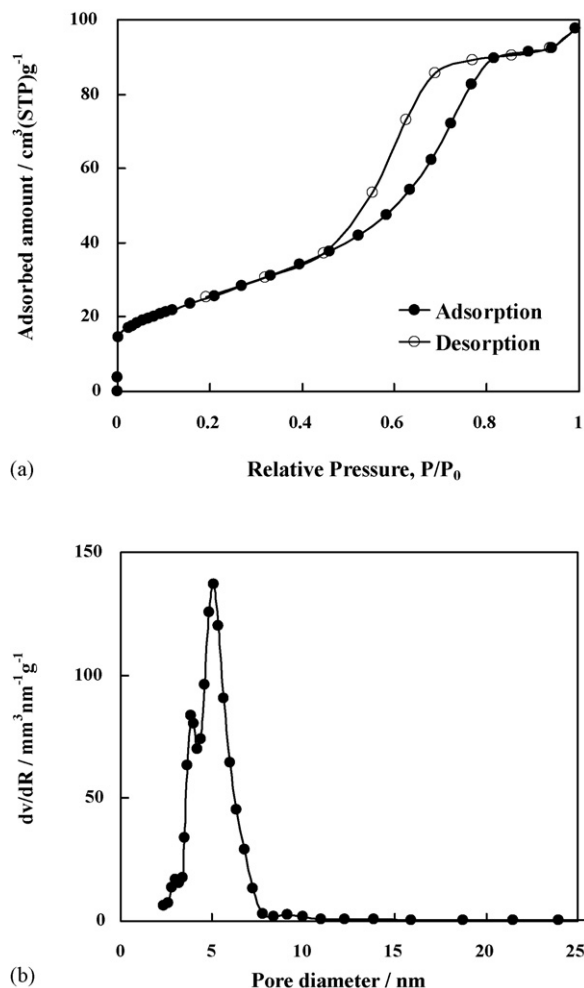


Fig. 1. N₂ adsorption–desorption isotherm (a) and pore size distribution (b) of the synthesized mesoporous Pt/TiO₂ photocatalyst.

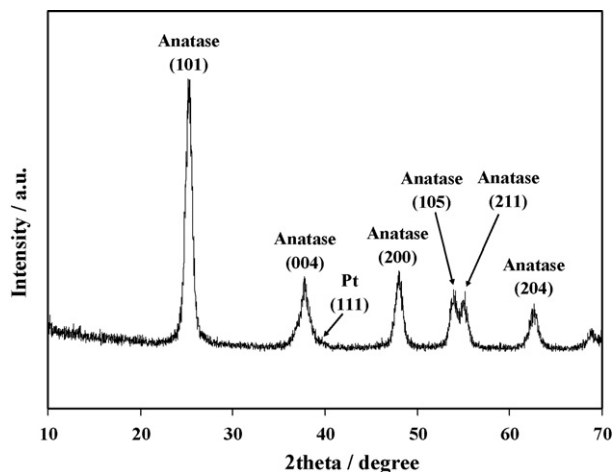


Fig. 2. XRD pattern of the synthesized mesoporous Pt/TiO₂ photocatalyst.

type of hysteresis loop. As can be seen from Fig. 1(b), a narrow monomodal pore size distribution, centered at a pore diameter in the mesopore region of 2–50 nm, can be obtained from the material synthesized by the synthesis system, suggesting its exquisite quality. The textural properties of the photocatalyst are listed as follows: BET surface area = 89 m² g⁻¹, mean pore diameter = 5.06 nm, and total pore volume = 0.162 cm³ g⁻¹.

The crystalline structure of the synthesized mesoporous Pt/TiO₂ photocatalyst revealed by XRD analysis is shown in

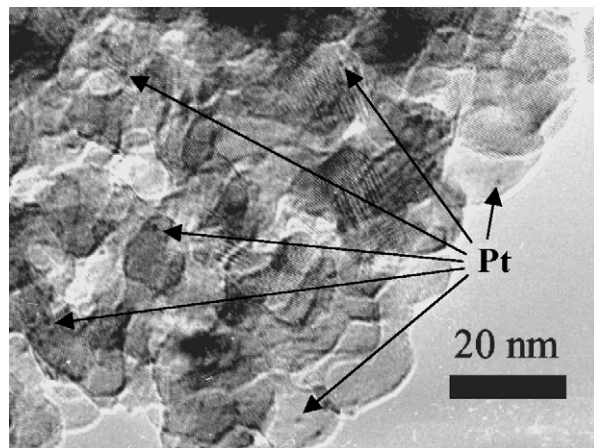


Fig. 3. TEM image of the synthesized mesoporous Pt/TiO₂ photocatalyst.

Fig. 2. The diffractogram is indexed to pure anatase TiO₂ (JCPDS Card no. 21-1272) [36] with high crystallinity. From the XRD result, the indistinguishable presence of the diffraction peaks of Pt indicates that the Pt particles were in a very high dispersion degree. As the minimum detection limit of the XRD technique is around 5 nm, it is inferred that the crystallite size of the Pt particles was below that value. The crystallite size of TiO₂ particles, estimated from line broadening of anatase (1 0 1) diffraction peak using Sherrer formula [37], was approx-

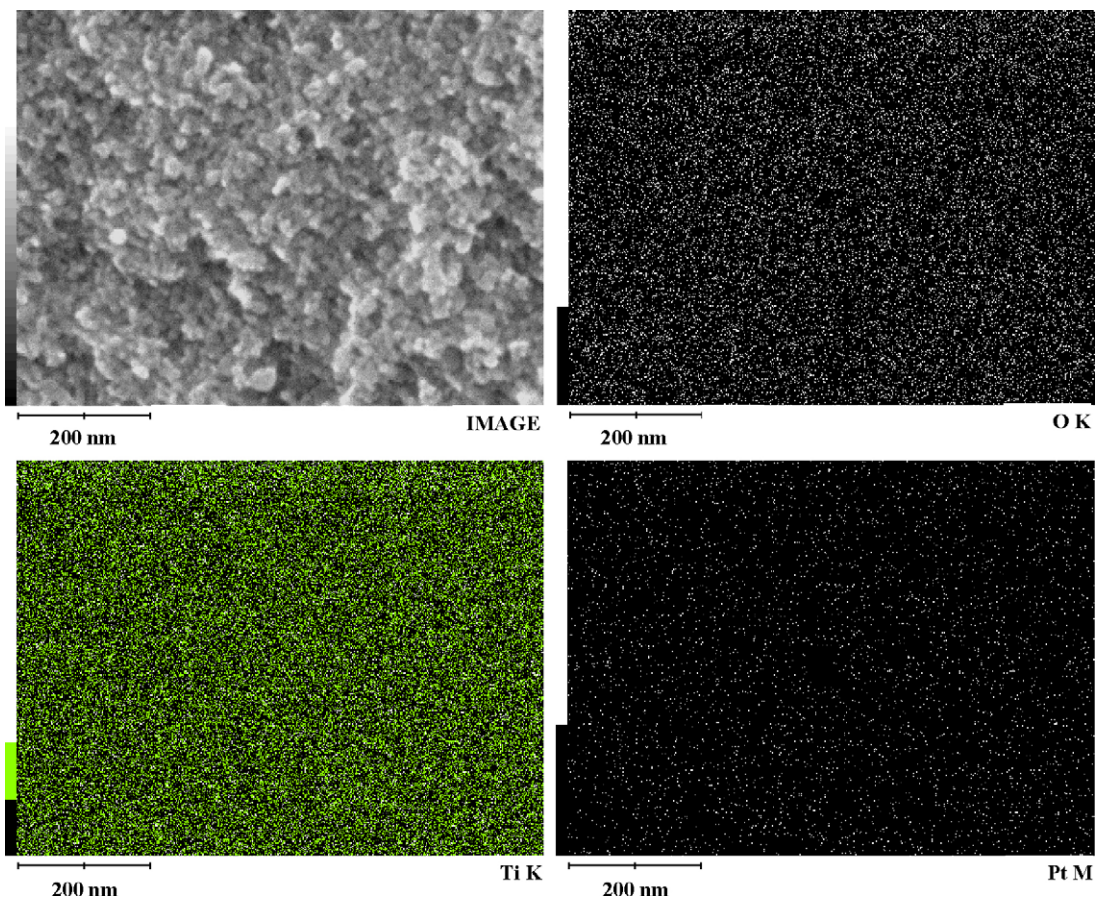


Fig. 4. SEM image and elemental mappings of the synthesized mesoporous Pt/TiO₂ photocatalyst.

imately 11 nm. The particle sizes of Pt and TiO₂ from the TEM analysis are in the region of 1–2 and 10–15 nm, respectively, as depicted by the TEM image in Fig. 3. The observed particle size of TiO₂ is in good accordance with the crystallite size calculated from the XRD result. In addition, homogeneously dispersed Pt nanoparticles on the TiO₂ surface are clearly seen from the TEM image.

The surface morphology of the synthesized photocatalyst was further investigated by using SEM. The acquired image is presented in Fig. 4. In the photocatalyst micrograph, particles with quite uniform size can be observed in aggregated clusters consisting of many nanoparticles. It can be seen that the photocatalyst was highly mesoporous, which is apparent by the SEM image. EDS analysis also provided useful information about the elemental distribution on the photocatalyst, as included in Fig. 4 by the elemental mapping of each component. The existence of dots in the elemental mapping images reveals the presence of all the investigated (Ti, O, and Pt) species. The EDS mappings reveal that all elements in the Pt-loaded TiO₂ were well distributed throughout the bulk photocatalyst, especially the investigated Pt species. This is another good verification of the high dispersion state of the deposited Pt nanoparticles. According to the N₂ adsorption–desorption, TEM, and SEM results, it is additionally worthwhile to emphasize that the mesoporous structure of the synthesized photocatalyst can be attributed to the pores formed between the nanocrystalline TiO₂ particles due to their aggregation, which is in the same line as the mesoporous TiO₂ reported in literature [38–43].

3.2. Photocatalytic H₂ evolution activity

3.2.1. Effect of sacrificial reagent type

In photocatalytic water splitting for H₂ evolution, the oxidation of water by holes is a much slower process than the reduction by electrons. In order to smooth the progress of the oxidation, sacrificial reagents or hole scavengers are often introduced, especially for the principal purpose of preventing the mutual electron–hole recombination process. Once the holes are scavenged from the photocatalyst surface, the longer decay time of surface electrons would certainly facilitate the reduction of

protons in the solution to form hydrogen on the Pt active sites [44–46]. It is also definitely important to first mention that no hydrogen evolution activity was experimentally observed for the blank tests (without photocatalyst or without sacrificial reagent).

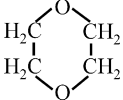
Initially, various types of sacrificial reagents were tested for the photocatalytic H₂ evolution to find which type of sacrificial reagent is the most effective in assisting the photocatalytic reaction. An aqueous solution containing the same amount of various sacrificial reagents was thus illuminated under identical reaction conditions. Table 1 shows the photocatalytic H₂ evolution activity of the synthesized nanocrystalline mesoporous Pt/TiO₂ photocatalyst using various sacrificial reagents, and Fig. 5 also shows the photocatalytic H₂ evolution profiles and activity using different sacrificial reagent types in an alcohol series. The results show that among the investigated sacrificial reagents, those in the alcohol series exhibited considerably higher photocatalytic activity than others. This might be attributable to the ease in donating lone-pair electrons to the valence band hole upon the photocatalyst excitation [47], as compared to other types of sacrificial reagents. Among the alcohol series itself, methanol was found to be the most effective and strongest sacrificial reagent to yield the highest photocatalytic H₂ evolution activity. It appears that compounds possessing very high polarity, such as acids and ketones, are unable to effectively suppress the electron–hole recombination, probably due to their stable electronic configuration. Apart from that, the carbon-to-carbon bond breaking also plays an important role in differentiating photocatalytic activity, since it directly involves the lone-pair electron donation. The extent of the carbon-to-carbon bond breaking decreases with the increase in chain elongation and complexity, as these factors contribute to enhance the steric hindrance in the molecule [47]. Since methanol was experimentally verified to be the most effective sacrificial reagent for the investigated system using the synthesized mesoporous Pt/TiO₂ photocatalyst, it was used as the main studied sacrificial reagent in further experiments.

3.2.2. Effect of initial solution pH

One of the important parameters affecting the photocatalytic reactions taking place on the photocatalyst surfaces is the solution pH, since it primarily dictates the surface charge properties

Table 1

Effect of various sacrificial reagent types on photocatalytic H₂ evolution activity of the synthesized mesoporous Pt/TiO₂ photocatalyst (reaction conditions: photocatalyst amount, 0.2 g; distilled water amount, 200 ml; sacrificial reagent amount, 20 ml; irradiation time, 5 h)

Type of sacrificial reagent	Molecular structure of sacrificial reagent	H ₂ evolution activity (μmol h ⁻¹)
Methanol	CH ₃ OH	1385
Ethanol	CH ₃ CH ₂ OH	1123
1-Propanol	CH ₃ CH ₂ CH ₂ OH	775
2-Propanol	CH ₃ CH(OH)CH ₃	599
1-Butanol	CH ₃ CH ₂ CH ₂ CH ₂ OH	629
Acetic acid	CH ₃ COOH	78
Acetone	CH ₃ COCH ₃	22
Ethylene glycol	OHCH ₂ CH ₂ OH	451
Diethylene dioxide (1,4-dioxane)		292
Dimethyl formamide	HCON(CH ₃) ₂	87

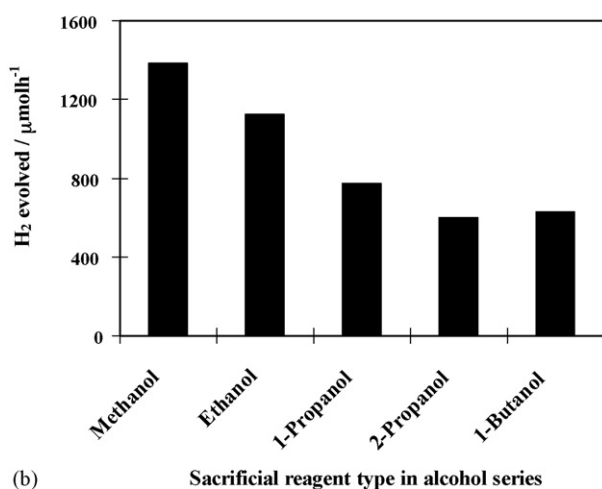
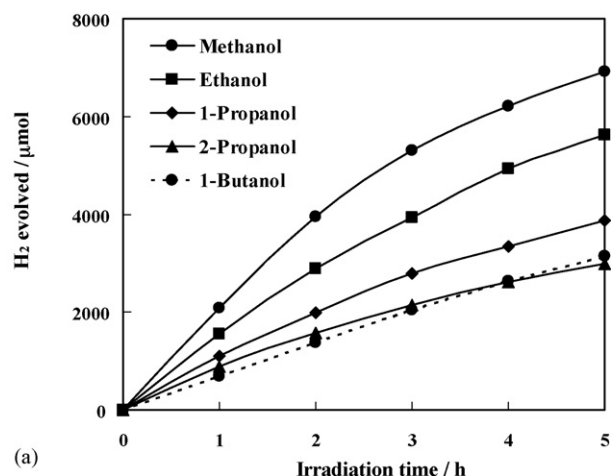


Fig. 5. Effect of sacrificial reagent type in alcohol series on (a) time course of H₂ evolved and (b) dependence of photocatalytic H₂ evolution activity of the synthesized mesoporous Pt/TiO₂ photocatalyst (reaction conditions: photocatalyst amount, 0.2 g; distilled water amount, 200 ml; sacrificial reagent amount, 20 ml; irradiation time, 5 h).

of the photocatalyst. In addition, the solution pH can affect the states of both reactant in solution and photocatalyst surface, which ultimately changes the electrostatic interaction between the reactant and the TiO₂ surface [48–50]. The role of initial solution pH on the photocatalytic H₂ evolution activity was studied over a broad pH range of 2–10.5 using methanol as a sacrificial reagent, noting that the initial pH of the original solution containing 200 ml distilled water and 20 ml methanol (2.25 M) is 5.8, and insignificant changes of solution pH were observed after the course of the photocatalytic reaction. The experimental results shown in Fig. 6 indicate that the efficiency of the H₂ evolution activity increases with an increase in solution pH from 2 to a range of 5–6, and a further increase in solution pH greater than 6 led to a drastic decrease in the H₂ evolution activity. The results imply that the H₂ evolution activity of the studied photocatalyst is favorable at mild acidic conditions, and the optimum initial solution pH is around 6.

The effect of solution pH on the efficiency of the photocatalytic H₂ evolution process is quite complicated since it

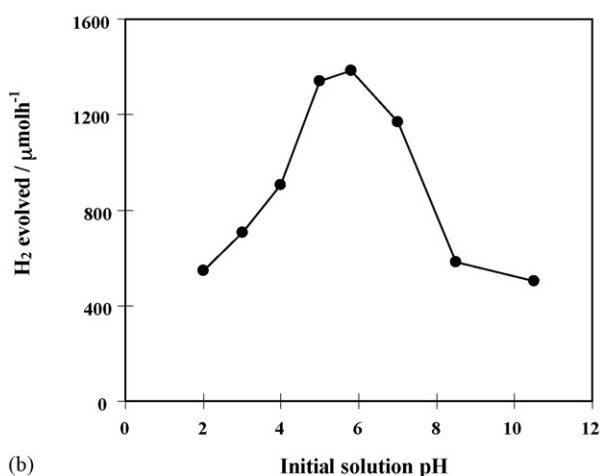
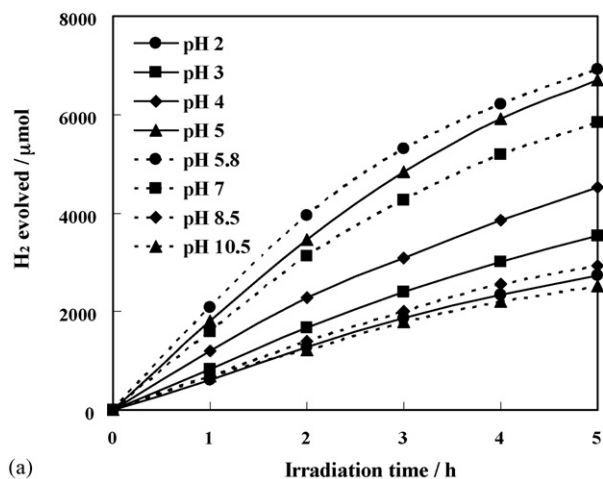
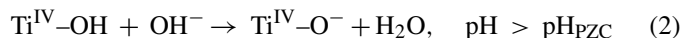
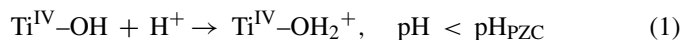


Fig. 6. Effect of initial solution pH on (a) time course of H₂ evolved and (b) dependence of photocatalytic H₂ evolution activity of the synthesized Pt/TiO₂ photocatalyst (reaction conditions: photocatalyst amount, 0.2 g; distilled water amount, 200 ml; sacrificial reagent type, methanol; sacrificial reagent amount, 20 ml; irradiation time, 5 h).

contributes to several roles. It is first related to the ionization state of the photocatalyst surface according to the following reactions:



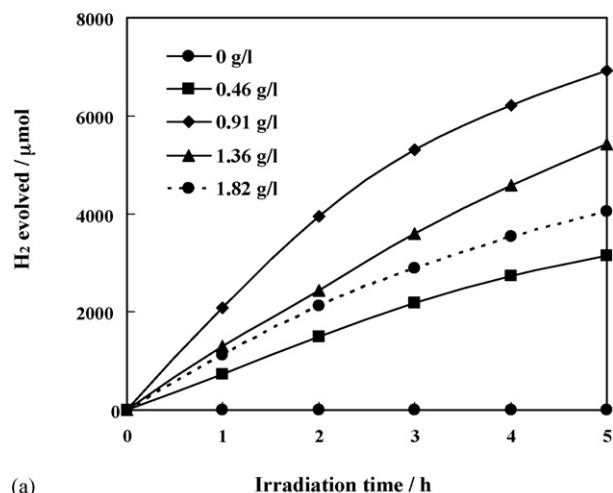
As known, a pH change can influence the adsorption of these species onto the TiO₂ photocatalyst surfaces, an important step for the photocatalytic reactions to take place. The point of zero charge (PZC) of the TiO₂ is approximately at pH 5.8–6.0 [51–53]. Therefore, at a pH < pH_{PZC}, the TiO₂ surface is positively charged, whereas at a pH > pH_{PZC}, the TiO₂ surface is negatively charged. At acidic pHs (pH < 5), an electrostatic repulsion between the positively charged surface of the photocatalyst and the hydronium cations (H⁺) present in the solution retards the adsorption of the hydronium cations so as to accordingly be reduced to form hydrogen, resulting in a lower photocatalytic H₂ evolution activity. In the opposite manner, at alkaline pHs (pH > 7), an electrostatic repulsion between the negatively charged surface of the photocatalyst

and the molecules of the sacrificial reagent (lone-pair electron donor) also inhibits the adsorption of the sacrificial reagent as to scavenge the valence band holes for preventing electron–hole recombination. Besides, the photogenerated electrons cannot easily transfer to the photocatalyst surface, plausibly because of the negative charge repulsion, and subsequently transfer to outer system via the photocatalytic reduction reaction. Therefore, the electrons moving inside the bulk photocatalyst have high probability to recombine with holes at both bulk trap and defect sites. A higher rate of mutual recombination also consequently results in a lower photocatalytic H₂ evolution activity. These basically imply that complicated interactions between the species/molecules and the photocatalyst are taking place at acidic or alkaline conditions. When the photocatalyst contains no charge, the species/molecules are probably allowed to much more easily reach the photocatalyst surface and achieve higher photocatalytic reaction activity [54,55], thus experimentally obtaining the highest H₂ evolution activity at the initial solution pHs near the point of zero charge.

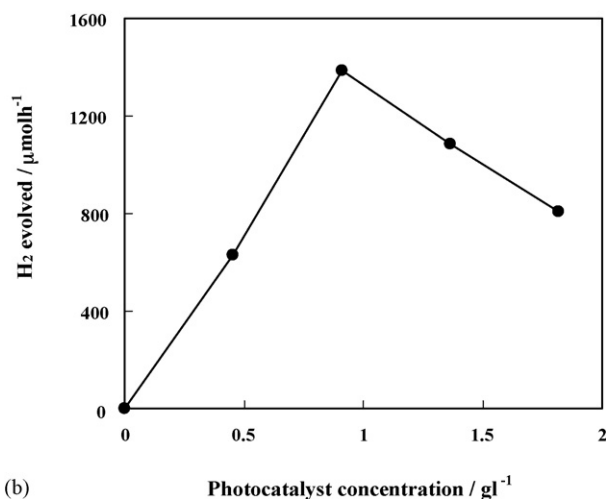
The TiO₂ particles, moreover, tend to agglomerate under acidic conditions [56]. This agglomeration can result in a lower surface area available for reactant adsorption and photon absorption, leading to a decrease in the photocatalytic activity; whereas another reason for the decrease in the photocatalytic activity under alkaline conditions can be attributed to the UV screening of the TiO₂ particles due to a higher concentration of OH[−] present in the solution [57]. Hence, the solution pH plays an important role both in the characteristics of reactant species-containing solutions and in the reaction mechanisms that can contribute to the H₂ evolution.

3.2.3. Effect of photocatalyst concentration

The effect of the concentration of the synthesized nanocrystalline mesoporous Pt/TiO₂ photocatalyst on the photocatalytic H₂ evolution was investigated in the range of 0–1.82 g l^{−1} by varying the amount of photocatalyst added to the reactor containing an original aqueous 2.25 M methanol solution (pH 5.8) without pH adjustment. Fig. 7 illustrates the photocatalytic H₂ evolution activity as a function of photocatalyst concentration. The H₂ evolution activity first increased and then decreased with an increase in the photocatalyst amount added to the reactor. A higher concentration of the photocatalyst is expected to correspond to a greater absorption of UV energy, leading to a higher photocatalytic H₂ evolution activity. However, the activity began to decline when the concentration of the photocatalyst exceeded 0.91 g l^{−1}, indicating that the addition of the photocatalyst has to be optimized. The obtained experimental results can be rationalized in terms of the availability of active sites on the TiO₂ surface and the light penetration of photoactivating light into the suspension. The availability of active sites increases with the increase in photocatalyst concentration in the suspension, but the light penetration and the consequent photoactivated volume of the suspension shrink [58]. The penetration of light is cloaked in the reactor by the large quantity of the photocatalyst in the aqueous solution. When the photocatalyst concentration is very high, after traveling a certain distance on an optical path, turbidity impedes the further penetration of light in the reactor, indicating



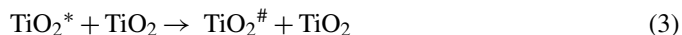
(a)



(b)

Fig. 7. Effect of photocatalyst concentration on (a) time course of H₂ evolved and (b) dependence of photocatalytic H₂ evolution activity of the synthesized mesoporous Pt/TiO₂ photocatalyst (reaction conditions: distilled water amount, 200 ml; sacrificial reagent type, methanol; sacrificial reagent amount, 20 ml; initial solution pH, 5.8; irradiation time, 5 h).

the block of the illuminating light. Although the light absorption of the outer photocatalyst increases, the capability of generating hydrogen from the inner photocatalyst decreases due to the lack of photoexcitation, signifying the screening effect of excess photocatalyst particles in the solution [49,59]. Consequently, the overall H₂ evolution activity decreases with a very high concentration of the photocatalyst. Moreover, the decrease in the photocatalytic activity at a higher photocatalyst concentration may be due to the deactivation of activated TiO₂ molecules by the collision with ground-state TiO₂ molecules (inactive TiO₂). The deactivation due to the shielding by TiO₂ can be explained according to the following reaction:



where TiO₂^{*} is the TiO₂ with active species adsorbed on its surface, and TiO₂[#] is the deactivated form of TiO₂ [60]. At a considerably high photocatalyst concentration, agglomeration and sedimentation of the photocatalyst particles have also been

reported. Under this condition, it leads to a reduction of the photocatalyst surface available for photon absorption and reactant adsorption, thus bringing lower stimulation to the photocatalytic reaction. An optimum photocatalyst concentration also greatly depends on the photoreactor geometry, the working conditions of the photoreactor, the degree of mixing, the UV lamp power, and the lamp geometry. The optimum amount of the photocatalyst has to be introduced into the system in order to avoid unnecessary excess photocatalyst and also to ensure total absorption of light photons for the efficient photocatalytic H_2 evolution reaction.

3.2.4. Effect of initial methanol concentration

It is important, both from mechanistic and application points of view, to study the dependence of the photocatalytic H_2 evolution reaction on the concentration of methanol, the most effective sacrificial reagent. The influence of initial methanol concentration on the photocatalytic H_2 evolution activity over the synthesized photocatalyst is shown in Fig. 8. With an increase in the methanol concentration, the photocatalytic activity dra-

matically increased and reached a maximum at the methanol concentration of 2.25 M. Beyond this optimum methanol concentration, a further increase in methanol concentration led to a decrease in the photocatalytic activity. Under the studied conditions, the optimum methanol concentration was about 2.25 M. At relatively high concentrations of methanol beyond the optimum point, although the surface active sites remain constant for a fixed catalyst concentration, the number of adsorbed methanol molecules accommodated on the photocatalyst surface increases [50,61]. Because the generation of valence band holes on the surface of the photocatalyst required for reacting with methanol molecules does not increase as the intensity of light and amount of catalyst are unchanged, there was an observed decrease in the photocatalytic H_2 evolution activity, probably due to the blockage of the adsorption of hydronium cations at surface active sites, so as to be reduced to produce hydrogen. Besides, as the photocatalytic reaction is an ion and radical reaction, and methanol can also somewhat behave as a quenching agent of ions and radicals [62], more ions and radicals can be quenched with the increase in methanol concentration. These mentioned reasons consequently lead to the decrease of H_2 evolution activity, after methanol concentration is over the optimum level.

3.2.5. Effect of irradiation time

The time courses of the photocatalytic H_2 evolution over the synthesized mesoporous Pt/TiO₂ photocatalyst at various reaction conditions are given in part (a) of Figs. 5–8. It can be clearly seen that under light radiation, with increasing the time of irradiation up to 5 h, the amount of H_2 evolved increased almost proportionally to the irradiation time in the investigated period. This is because, with an increase in irradiation time, the photons absorbed on the surface of the photocatalyst become greater, which, in turn, helps in the photocatalytic process. However, a slight decrease in the H_2 evolution rate at a long irradiation time was observed. This can be explained that in a photocatalytic batch system, a long irradiation time regularly causes a progressive decline in the H_2 evolution rate due to the back reactions of products generated in the reaction system, as well as the pressure buildup in the gas phase [63]. Additionally, the active site deactivation due to the strong absorption of some molecular species might also be another cause of the decrease in the H_2 evolution activity after a long illumination time [58].

4. Conclusions

The use of SSSG-prepared 0.6 wt% Pt-loaded nanocrystalline mesoporous TiO₂ photocatalyst with high surface area and narrow monomodal pore size distribution for photocatalyzing H_2 evolution from water was studied under various reaction conditions. Several operational parameters were investigated in order to determine the optimum conditions exhibiting the maximum H_2 evolution activity. The experimental results showed that methanol was found to be the most efficient sacrificial reagent among several types of sacrificial reagents investigated. Mild acidic pH values in the range of 5–6 were favorable for the reaction. The optimum photocatalyst and initial methanol concentration were found to be 0.91 g l⁻¹ and 2.25 M, respectively.

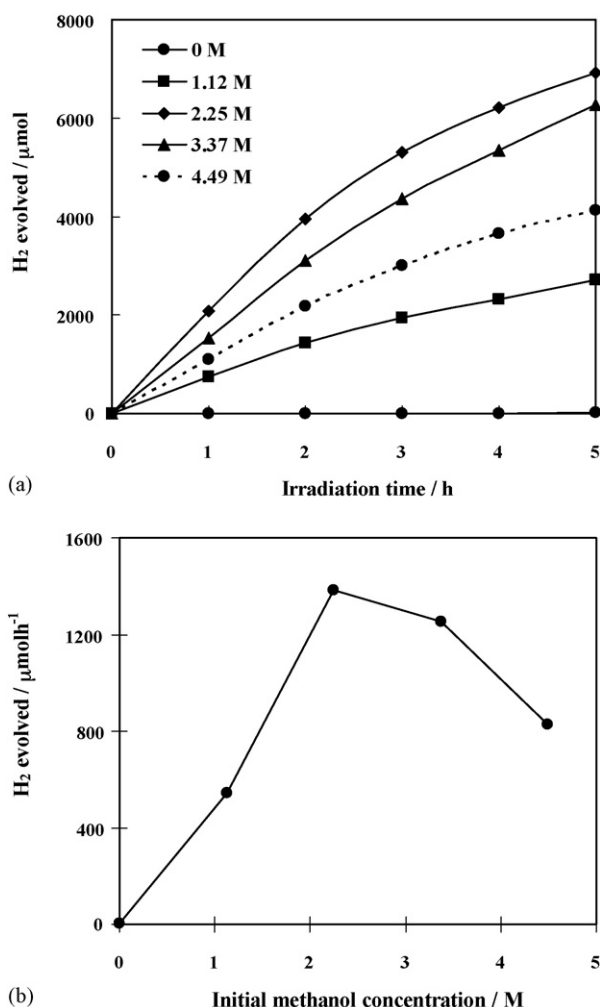


Fig. 8. Effect of initial methanol concentration on (a) time course of H_2 evolved and (b) dependence of photocatalytic H_2 evolution activity of the synthesized mesoporous Pt/TiO₂ photocatalyst (reaction conditions: photocatalyst amount, 0.2 g; solvent: distilled water; sacrificial reagent type, methanol; total solution volume, 220 ml; initial solution pH, 5.8; irradiation time, 5 h).

Acknowledgements

This work was financially supported by grants provided to the first/corresponding author by the Thailand Research Fund (TRF) (Contract/Grant No. MRG4980030) and by Chulalongkorn University, Thailand, through the Grants for Development of New Faculty Staff under the Ratchadapisek Somphot Endowment Fund (Contract/Grant No. 100/2549). The partial supports from the Petroleum and Petrochemical Consortium under the Ministry of Education, Thailand, and the Research Unit of Petrochemical and Environmental Catalysis under the Ratchadapisek Somphot Endowment Fund, Chulalongkorn University, Thailand, are also greatly acknowledged.

References

- [1] M.A. Fox, M.T. Dulay, *Chem. Rev.* 93 (1993) 341–357.
- [2] O. Legrini, E. Oliveros, A.M. Braun, *Chem. Rev.* 93 (1993) 671–698.
- [3] J.C. Amphlett, K.A.M. Creber, J.M. Davis, R.F. Mann, B.A. Peppley, D.M. Stokes, *Int. J. Hydrogen Energy* 19 (1994) 131–137.
- [4] M.R. Hoffmann, S.T. Martin, W. Choi, D. Bahnemann, *Chem. Rev.* 95 (1995) 69–96.
- [5] K. Rajashwer, *J. Appl. Electrochem.* 25 (1995) 1067–1082.
- [6] M.I. Litter, *Appl. Catal. B: Environ.* 23 (1999) 89–114.
- [7] T. Sakata, T. Kawai, K. Hashimoto, *Chem. Phys. Lett.* 88 (1982) 50–54.
- [8] J. Abrahams, R.S. Davidson, C.L. Morrison, *J. Photochem.* 29 (1985) 353–361.
- [9] G.R. Bamwenda, S. Tsubota, T. Nakamura, M. Haruta, *J. Photochem. Photobiol. A: Chem.* 89 (1995) 177–189.
- [10] T. Abe, E. Suzuki, K. Nagoshi, K. Miyashita, M. Kaneko, *J. Phys. Chem. B* 103 (1999) 1119–1123.
- [11] Y. Li, G. Lu, S. Li, *Chemosphere* 52 (2003) 843–850.
- [12] N.L. Wu, M.S. Lee, *Int. J. Hydrogen Energy* 29 (2004) 1601–1605.
- [13] T. Sreethawong, Y. Suzuki, S. Yoshikawa, *J. Solid State Chem.* 178 (2005) 329–338.
- [14] T. Sreethawong, Y. Suzuki, S. Yoshikawa, *Int. J. Hydrogen Energy* 30 (2005) 1053–1062.
- [15] T. Sreethawong, S. Ngamsinlapasathian, Y. Suzuki, S. Yoshikawa, *J. Mol. Catal. A: Chem.* 235 (2005) 1–11.
- [16] T. Sreethawong, S. Yoshikawa, *Catal. Commun.* 6 (2005) 661–668.
- [17] A. Fujishima, K. Honda, *Nature* 238 (1972) 37–38.
- [18] A. Linsebigler, G. Lu, J.T. Yates, *Chem. Rev.* 95 (1995) 735–758.
- [19] E. Borgarello, J. Kiwi, M. Graetzel, E. Pelizzetti, M. Visca, *J. Am. Chem. Soc.* 104 (1982) 2996–3002.
- [20] W. Choi, A. Termin, M.R. Hoffmann, *J. Phys. Chem.* 98 (1994) 13669–13679.
- [21] X. Fu, L.A. Clark, Q. Yang, M.A. Anderson, *Environ. Sci. Technol.* 30 (1995) 647–653.
- [22] C. Anderson, A.J. Bard, *J. Phys. Chem.* 99 (1995) 9882–9885.
- [23] K.T. Ranjit, H. Cohen, I. Willner, S. Bossmann, A. Braun, *J. Mater. Sci.* 34 (1999) 5273–5280.
- [24] J. Moon, H. Takagi, F. Fujishiro, M. Awano, *J. Mater. Sci.* 36 (2001) 949–955.
- [25] V. Vamathevan, R. Amal, D. Beydoun, G. Low, S. Mcevoy, *J. Photochem. Photobiol. A: Chem.* 148 (2002) 233–245.
- [26] Y. Li, T. Wang, S. Peng, G. Lu, S. Li, *Acta Phys.-Chim. Sin.* 20 (2004) 1434–1439.
- [27] N. Serpone, E. Pelizzetti, *Photocatalysis: Fundamentals and Applications*, Wiley, New York, 1989.
- [28] N. Serpone, R.F. Khairutdinov, *Semiconductor Nanoclusters, Physical, Chemical, and Catalytic Aspects*, Elsevier Science, Amsterdam, 1997.
- [29] D.M. Antonelli, Y.J. Ying, *Angew. Chem. Int. Ed. Engl.* 34 (1995) 2014–2017.
- [30] D.M. Antonelli, *Micropor. Mesopor. Mater.* 30 (1999) 315–319.
- [31] P. Yang, D. Zhao, D.I. Margolese, B.F. Chmelka, G.D. Stucky, *Chem. Mater.* 11 (1999) 2813–2826.
- [32] H. Yoshitake, T. Sugihara, T. Tatsumi, *Chem. Mater.* 14 (2002) 1023–1029.
- [33] V. Idakiev, T. Tabakova, Z.Y. Yuan, B.L. Su, *Appl. Catal. A: Gen.* 270 (2004) 135–141.
- [34] T. Sreethawong, S. Yoshikawa, *Int. J. Hydrogen Energy* 31 (2006) 786–796.
- [35] F. Rouquerol, J. Rouquerol, K. Sing, *Adsorption by Powders and Porous Solids: Principles, Methodology and Applications*, Academic Press, San Diego, 1999.
- [36] J.V. Smith (Ed.), *X-ray Powder Data File*, American Society for Testing Materials, 1960.
- [37] B.D. Cullity, *Elements of X-ray Diffraction*, Addison-Wesley Publication Company, Massachusetts, 1978.
- [38] J. Yu, J.C. Yu, M.K.P. Lueng, W. Ho, B. Cheng, X. Zhao, J. Zhao, *J. Catal.* 217 (2003) 69–78.
- [39] J.C. Yu, J. Yu, W. Ho, L. Zhang, *Chem. Commun.* 19 (2001) 1942–1943.
- [40] Y. Zhang, A. Weidenkaff, A. Reller, *Mater. Lett.* 54 (2002) 375–381.
- [41] Y. Zhang, H. Zhang, Y. Xu, Y. Wang, *J. Solid State Chem.* 177 (2004) 3490–3498.
- [42] Y.V. Kolen'ko, V.D. Maximov, A.V. Garshev, P.E. Meskin, N.N. Oleynikov, B.R. Churagulov, *Chem. Phys. Lett.* 388 (2004) 411–415.
- [43] Q. Sheng, Y. Cong, S. Yuan, J. Zhang, M. Anpo, *Micropor. Mesopor. Mater.* 95 (2006) 220–225.
- [44] J. Kiwi, M. Grätzel, *J. Phys. Chem.* 88 (1984) 6146–6152.
- [45] A. Mills, S. Le Hunte, *J. Photochem. Photobiol. A: Chem.* 108 (1997) 1–35.
- [46] D.W. Hwang, H.G. Kim, J. Kim, K.Y. Cha, Y.G. Kim, J.S. Lee, *J. Catal.* 193 (2000) 40–48.
- [47] A. Hameed, M.A. Gondal, *J. Mol. Catal. A: Chem.* 233 (2005) 35–41.
- [48] F.L. Palmer, B.R. Eggins, H.M. Coleman, *J. Photochem. Photobiol. A: Chem.* 148 (2002) 137–143.
- [49] S. Lathasree, A.N. Rao, B. Sivasankar, V. Sadasivam, K. Rengaraj, *J. Mol. Catal. A: Chem.* 223 (2004) 101–105.
- [50] D.P. Das, K. Parida, B.R. De, *J. Mol. Catal. A: Chem.* 240 (2005) 1–6.
- [51] G.A. Parks, *Chem. Rev.* 65 (1965) 177–198.
- [52] W.H. Van Riemsdijk, G.H. Bolt, L.K. Koopal, J. Blaakmeer, *J. Colloid Interf. Sci.* 109 (1986) 219–228.
- [53] Colloidal Dynamics Inc., ZetaProbe Application, Determining the Isoelectric Point (IEP), Colloidal Dynamics, Colloidal Dynamics Inc., Warwick, Rhode Island, USA, 2002 (available at <http://www.colloidal-dynamics.com>).
- [54] D.S. Bhatkhande, V.G. Pangarkar, A.A.M.C. Beenackers, *J. Chem. Technol. Biotechnol.* 77 (2001) 102–116.
- [55] E. Evgenidou, K. Fytianos, I. Poullos, *J. Photochem. Photobiol. A: Chem.* 175 (2005) 29–38.
- [56] M.H. Habibi, A. Hassanzadeh, S. Mahdavi, *J. Photochem. Photobiol. A: Chem.* 172 (2005) 89–96.
- [57] A. Mills, R.H. Davies, D. Worsley, *Chem. Soc. Rev.* 22 (1993) 417–425.
- [58] I.K. Konstantinou, T.A. Albanis, *Appl. Catal. B: Environ.* 49 (2004) 1–14.
- [59] T. Sehilli, P. Boule, J. Lemaire, *J. Photochem. Photobiol. A: Chem.* 50 (1989) 117–127.
- [60] B. Neppolian, H.C. Choi, S. Sakthivel, B. Arabindoo, V. Murugesan, *J. Hazard. Mater.* 89 (2002) 303–317.
- [61] M. Qamar, M. Muneer, *J. Hazard. Mater.* 120 (2005) 219–227.
- [62] W. Cui, L. Feng, C. Xu, S. Lü, F. Qiu, *Catal. Commun.* 5 (2004) 533–536.
- [63] K.E. Karakitsou, X.E. Verykios, *J. Catal.* 134 (1992) 629–634.